Electronic Supplementary Information

Thermo-responsive hybrid "hairy-rod" polypeptides for smart antitumor drug delivery

Jianxun Ding,[a] Li Zhao,[ab] Di Li,[a] Chunsheng Xiao,*[a] Xiuli Zhuang,*[a] Xuesi Chen[a]

[a]Key Laboratory of Polymer Ecomaterials, Changchun Institute of Applied Chemistry, Chinese Academy of Sciences, Changchun 130022, P. R. China. Fax: +86 431 85262367; Tel: +86 431 85262367; E-mail: xiaocs@ciac.jl.cn; zhuangxl@ciac.jl.cn
[b]Graduate University of Chinese Academy of Sciences, Beijing 100039, P. R. China

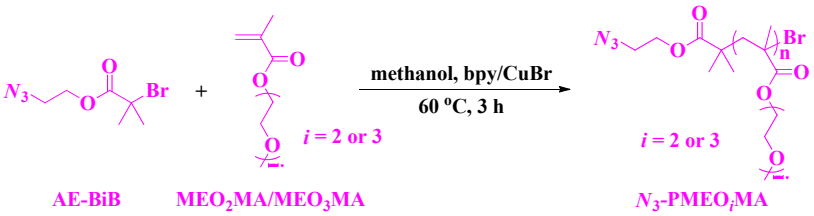

Scheme S1 Synthetic route to N_3-PMEO$_i$MA.

Table S1 Characterizations of N_3-PMEO$_i$MA.

Entry	Feeding Molar Ratio of MEO_2MA, MEO_3MA/Br	DP of MEO_2MA/ MEO_3MA[a]	M_n[a] (g mol^{-1})	M_n[b] (g mol^{-1})	PDI[b]
N_3-PMEO_2MA_{27}	50, 0	27/0	5300	5900	1.18
N_3-P(MEO_2MA_{18}-*co*-MEO_3MA_9)	35, 15	18/9	5700	6300	1.20
N_3-P(MEO_2MA_{13}-*co*-MEO_3MA_{13})	25, 25	13/13	5700	6000	1.19
N_3-P(MEO_2MA_7-*co*-MEO_3MA_{18})	15, 35	7/18	5700	6200	1.23
N_3-PMEO_3MA_{26}	0, 50	0/26	6300	6800	1.19

[a] Determined by ^{1}H NMR. [b] Determined by GPC.

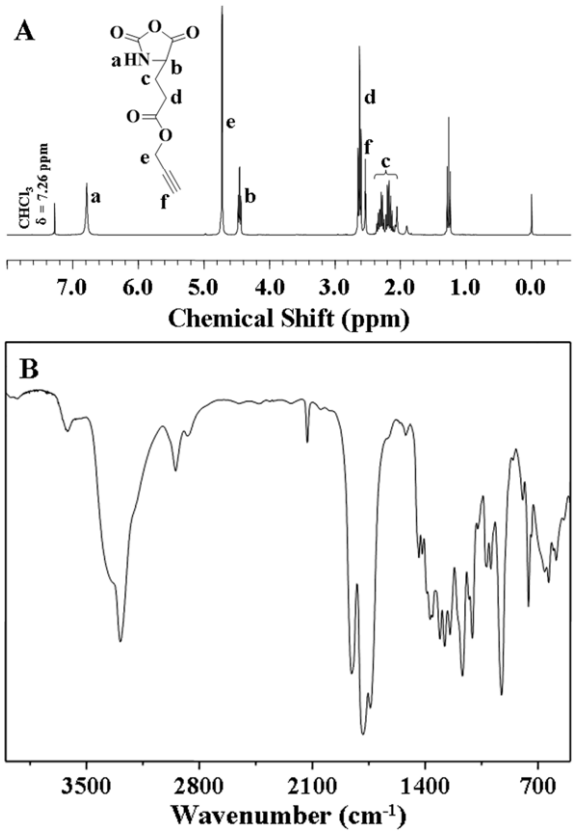

Fig. S1 ^{1}H NMR (in $CDCl_3$) (A) and FT-IR (B) spectra of PLG NCA.

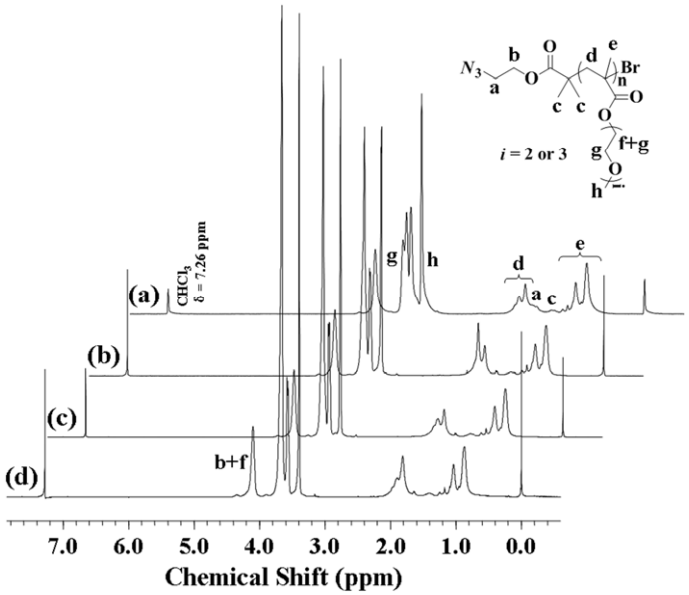

Fig. S2 ^{1}H NMR spectra of N_3-PMEO$_2$MA$_{27}$ (a), N_3-P(MEO$_2$MA$_{18}$-*co*-MEO$_3$MA$_9$) (b), N_3-P(MEO$_2$MA$_7$-*co*-MEO$_3$MA$_{18}$) (c) and N_3-PMEO$_3$MA$_{26}$ (d) (in $CDCl_3$).

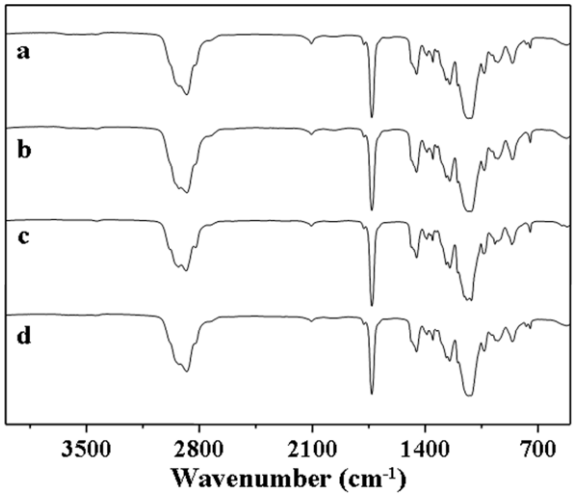

Fig. S3 FT-IR spectra of N_3-PMEO$_2$MA$_{27}$ (a), N_3-P(MEO$_2$MA$_{18}$-*co*-MEO$_3$MA$_9$) (b), N_3-P(MEO$_2$MA$_7$-*co*-MEO$_3$MA$_{18}$) (c) and N_3-PMEO$_3$MA$_{26}$ (d).

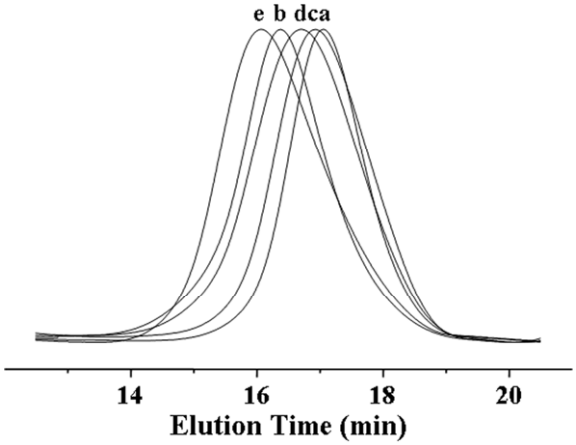

Fig. S4 GPC chromatograms of N_3-PMEO$_2$MA$_{27}$ (a), N_3-P(MEO$_2$MA$_{18}$-*co*-MEO$_3$MA$_9$) (b), N_3-P(MEO$_2$MA$_{13}$-*co*-MEO$_3$MA$_{13}$) (c), N_3-P(MEO$_2$MA$_7$-*co*-MEO$_3$MA$_{18}$) (d) and N_3-PMEO$_3$MA$_{26}$ (e) with THF as eluent.

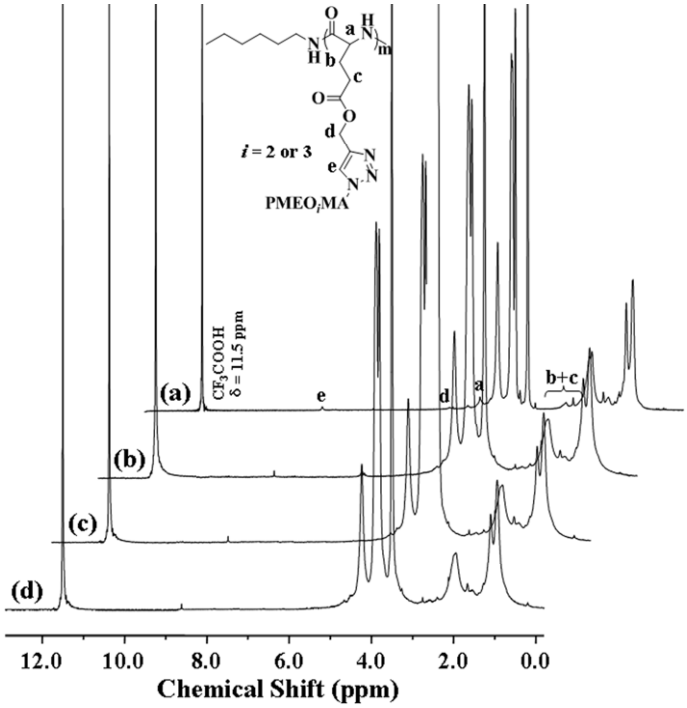

Fig. S5 ^{1}H NMR spectra of **P1** (a), **P2** (b), **P4** (c) and **P5** (d) (in CF_3COOD).

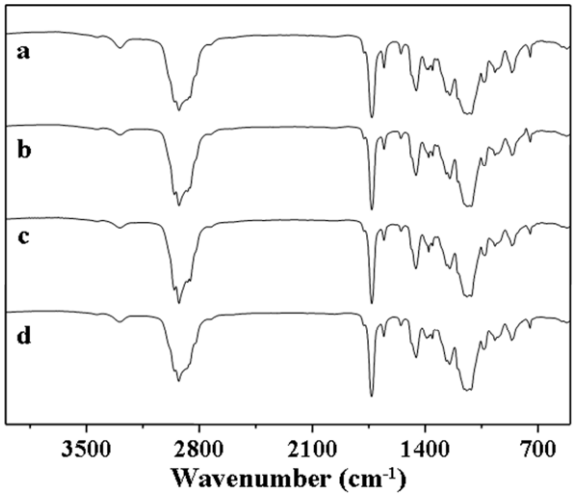

Fig. S6 FT-IR spectra of **P1** (a), **P2** (b), **P4** (c) and **P5** (d).

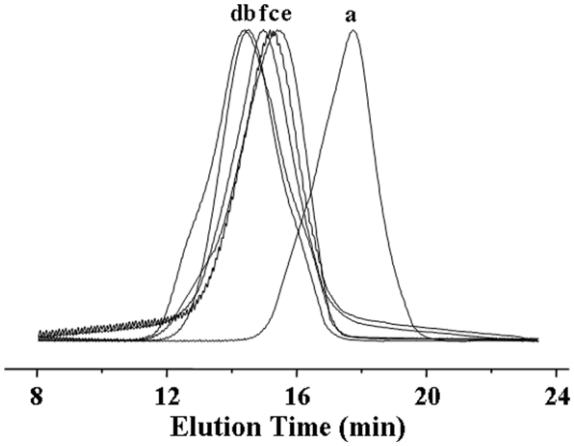

Fig. S7 GPC chromatograms of $PPLG_{40}$ (a), **P1** (b), **P2** (c), **P3** (d), **P4** (e) and **P5** (f) with DMF as eluent.

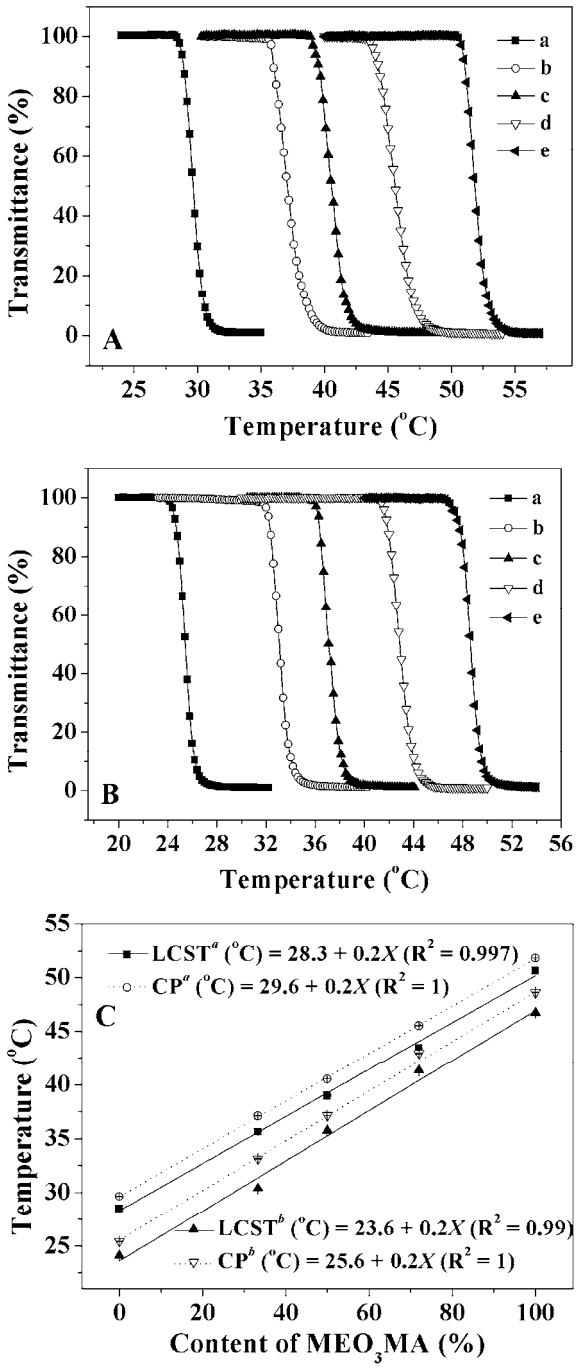

Fig. S8 Thermo-responsive behaviors of N_3-PMEO$_2$MA$_{27}$ (a), N_3-P(MEO$_2$MA$_{18}$-*co*-MEO$_3$MA$_9$) (b), N_3-P(MEO$_2$MA$_{13}$-*co*-MEO$_3$MA$_{13}$) (c), N_3-P(MEO$_2$MA$_7$-*co*-MEO$_3$MA$_{18}$) (d) and N_3-PMEO$_3$MA$_{26}$ (e) in deionized water (A) and physiological saline (B), and LCST and CP as a function of MEO$_3$MA content in deionized water (a) and physiological saline (b) (C).

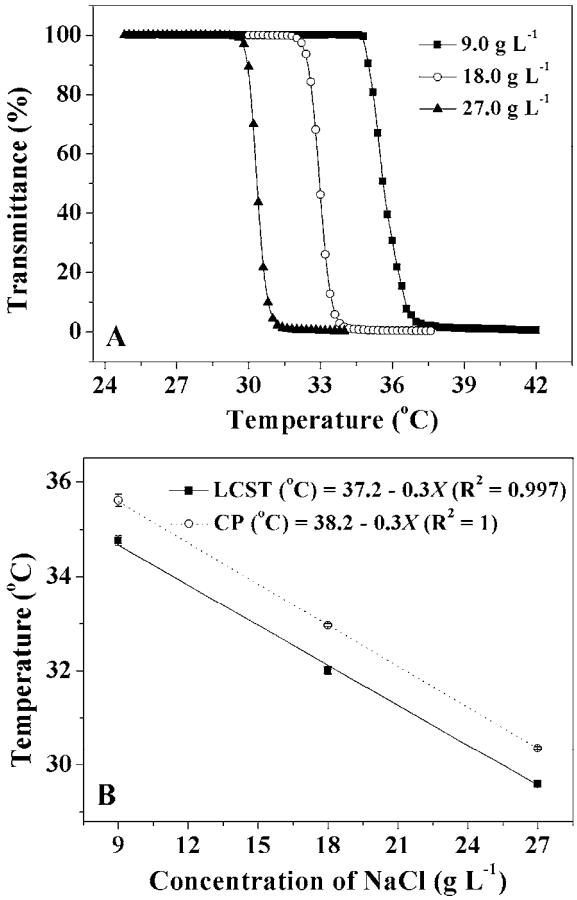

Fig. S9 Thermo-responsive behaviors of **P4** in 9.0, 18.0 and 27.0 g L^{-1} aqueous sodium chloride (NaCl) (A), and LCST and CP as a function of NaCl concentration (B).

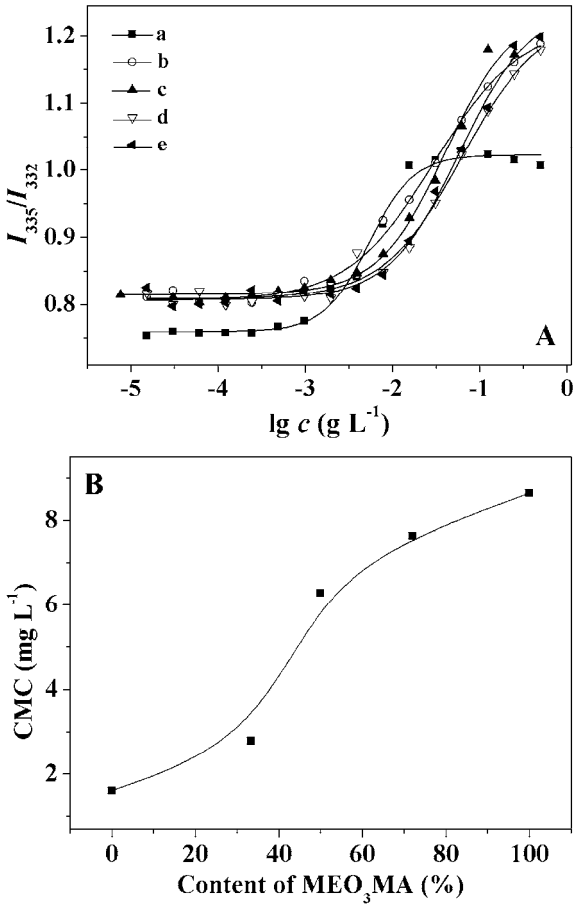

Fig. S10 The intensity ratio (I_{335}/I_{332}) as a function of logarithm of **P1** (a), **P2** (b), **P3** (c), **P4** (d) or **P5** concentration (e) (A), and CMC value as a function of MEO_3MA content in PBS (B).